Received: 19 May 2020 | Revised: 28 June 2020 | Accepted: 8 July 2020

DOI: 10.1096/fj.202001249R

RESEARCH ARTICLE

THE FASEB JOURNAL

Interleukin-8 drives CD38 to form NAADP from $NADP^+$ and NAAD in the endolysosomes to mobilize Ca^{2+} and effect cell migration

Tae-Sik Nam[1] | **Dae-Ryoung Park**[1] | **So-Young Rah**[1] | **Tae-Gyu Woo**[1] | **Hun Taeg Chung**[2] | **Charles Brenner**[3] | **Uh-Hyun Kim**[1]

[1]Department of Biochemistry & National Creative Research Laboratory for Ca^{2+} Signaling, Chonbuk National University Medical School, Jeonju, Korea

[2]Department of Biological Sciences, University of Ulsan, Ulsan, Korea

[3]Department of Biochemistry, University of Iowa, Iowa City, IA, USA

Correspondence
Charles Brenner, Department of Biochemistry, University of Iowa, Iowa City, IA 52242, USA.
Email: charles-brenner@uiowa.edu

Uh-Hyun Kim, Department of Biochemistry, Chonbuk National University, Medical School, Keum-am dong, Jeonju 561-182, Republic of Korea.
Email: uhkim@chonbuk.ac.kr

Funding information
National Research Foundation of Korea (NRF), Grant/Award Number: 2012R1A3A2026453, 2014R1A6A1030318 and 2012R1A3A2026453; Roy J. Carver Trust

Abstract

Nicotinic acid adenine dinucleotide phosphate (NAADP) is the most potent Ca^{2+} mobilizing second messenger whose formation has remained elusive. In vitro, CD38-mediated NAADP synthesis requires an acidic pH and a nonphysiological concentration of nicotinic acid (NA). We discovered that CD38 catalyzes synthesis of NAADP by exchanging the nicotinamide moiety of nicotinamide adenine dinucleotide phosphate ($NADP^+$) for the NA group of nicotinic acid adenine dinucleotide (NAAD) inside endolysosomes of interleukin 8 (IL8)-treated lymphokine-activated killer (LAK) cells. Upon IL8 stimulation, cytosolic $NADP^+$ is transported to acidified endolysosomes via connexin 43 (Cx43) and gated by cAMP-EPAC-RAP1-PP2A signaling. CD38 then performs a base-exchange reaction with the donor NA group deriving from NAAD, produced by newly described endolysosomal activities of NA phosphoribosyltransferase (NAPRT) and NMN adenyltransferase (NMNAT) 3. Thus, the membrane organization of endolysosomal CD38, a signal-mediated transport system for $NADP^+$ and luminal NAD^+ biosynthetic enzymes integrate signals from a chemokine and cAMP to specify the spatiotemporal mobilization of Ca^{2+} to drive cell migration.

KEYWORDS
calcium, cell migration, nicotinamide adenine dinucleotide, signal transduction

Abbreviations: Cx43, connexin 43; EPAC, cAMP-regulated guanine nucleotide exchange factor II; HPLC, high pressure liquid chromatography; IDO, indoleamine 2,3 dioxygenase; IL8, interleukin 8; KD, knockdown; LAK, lymphokine-activated killer; LC-MS/MS, liquid chromatography-tandem mass spectrometry; NA, nicotinic acid; NAADP, nicotinic acid adenine dinucleotide phosphate; NADP+, nicotinamide adenine dinucleotide phosphate; NAM, nicotinamide; NAD+, nicotinamide adenine dinucleotide; NAAD, nicotinic acid adenine dinucleotide; NAMN, nicotinic acid mononucleotide; NMN, nicotinamide mononucleotide; NMNAT, NAMN/NMN adenyltransferase; NAPRT, NA phosphoribosyltransferase; OA, okadaic acid; PMSF, phenylmethylsulfonyl fluoride; PP2A, protein phosphatase 2A; PKG, protein kinase G; QPRT, quinolinic acid phosphoribosyltransferase; Rap1, Ras-related protein 1; RT-PCR, reverse transcription polymerase chain reaction; siRNA, small interference RNA; V-ATPase, vacuolar (H+)-ATPases.

Tae-Sik Nam and Dae-Ryoung Park are the authors contributed equally to this work.

1 | INTRODUCTION

Ca^{2+} mobilization from acidic intracellular stores is mediated by formation of nicotinic acid adenine dinucleotide phosphate (NAADP),[1,2] a metabolite related to nicotinamide adenine dinucleotide phosphate ($NADP^+$) that can be formed in vitro by the membrane-associated CD38 protein performing a nucleobase exchange reaction between the nicotinamide (NAM) moiety of $NADP^+$ and free nicotinic acid (NA) at acidic pH.[3,4] NAADP formation is stimulated by diverse stimuli including receptor binding and cell contact.[5,6] In turn, high affinity release of Ca^{2+} from acidic compartments mediates subsequent release of Ca^{2+} from the endoplasmic reticulum that is required for mobility, differentiation, immune, and contractile functions in plant and animal tissues.[7] CD38 adopts two membrane orientations across multiple membrane compartments,[8] and they produce two additional nicotinamide adenine dinucleotide (NAD^+)-related compounds: cyclic ADP-ribose and ADP-ribose.[9,10] However, NA is generally considered a bacterial NAD^+ metabolite without appreciable availability in NAADP producing cells.[11] Due to this abstruse backdrop, the substrates utilized by CD38 as well as how those substrates and CD38 are transiently colocalized to affect signal-dependent NAADP production have remained elusive.

In lymphokine-activated killer (LAK) cells, binding of interleukin 8 (IL8) to its G-protein coupled receptor, CXCR1, leads to activation of guanylyl cyclase and protein kinase G (PKG), which leads to internalization of CD38 and cADPR production.[9,10] In turn, cAMP is produced followed by formation of NAADP in lysosome-related acidic organelles, resulting in IL8-driven cell migration in a manner that depends on EPAC, protein kinase A and RAP1.[12]

Here, we used cell fractionation to identify and reconstitute signal-dependent, CD38-dependent and $NADP^+$-dependent production of NAADP. Here, we show that IL8 causes association of vacuolar (H^+)-ATPases (V-ATPase) and a cAMP-EPAC-RAP1-PP2A-mediated activation of connexin 43 (Cx43) to transport $NADP^+$ into the lumen of endolysosomes. The other CD38 substrate is here identified as nicotinic acid adenine dinucleotide (NAAD) produced by endolysosomal activities of NA phosphoribosyltransferase and NMN adenyltransferase 3. Compartmentalization of NAAD synthesis and signal-mediated acidification and transfer of $NADP^+$ are thereby required to form NAADP and transmit signals for Ca^{2+} mobilization.

2 | MATERIALS AND METHODS

2.1 | Animals

C57BL/6 mice were purchased from Orient (Seongnam Korea). Mice were inbred and kept in animal facilities at Chonbuk National University Medical School under specific pathogen-free conditions. All studies conformed to the Guide for the Care and Use of Laboratory Animals published by the US National Institutes of Health (NIH Publication No. 85-23, revised 1996). The entire project was reviewed and approved by the Institutional Animal Care and Use Committee of the Chonbuk National University Medical School (CBNU 2018-069).

2.2 | preparation of Lak cells

LAK cells were prepared as described previously.[9,12] Briefly, spleens of mice were minced harvested. RBCs were lysed by incubation with RBC lysis buffer (0.15 M NH_4Cl, 10 mM $KHCO_3$, 0.1 mM EDTA, pH 7.2) and the cells were thereafter washed with serum-free RPMI1640 twice. The RBC-removed cell preparations were incubated on a nylon-wool column at 37°C for 1 hours in a 5% CO_2 incubator to remove B lymphocytes and macrophages. Nylon-wool nonadherent cells were collected and incubated at 2×10^6 cells/mL density in a culture media containing 3000 IU/mL IL2 in a 5% CO_2 incubator at 37°C. Culture media was RPMI 1640 supplemented with 10% FBS, 0.25 μg/mL amphotericin B, 10 U/mL penicillin G, 100 μg/mL streptomycin, 1 mM L-glutamine, 1% nonessential amino acids, and 50 μM 2-mercaptoethanol. After incubation for 4 days, floating cells were removed, and adherent cells were cultured in the same media containing 3000 IU/mL IL2. LAK cells induced by IL2 for 8-10 days were used throughout the study.

2.3 | Subcellular Fractionation of Lak cells and Western blotting

Organelles were separated as described.[12] LAK cells were homogenized with a 30G syringe in 1 mL of a solution consisting of 0.25 M sucrose, 10 mM HEPES, pH 7.4 and 1 mM PMSF (homogenate buffer). The homogenate was then centrifuged at 1000 ×*g* for 10 minutes at 4°C and the supernatant was loaded on the top of a continuous 0.4-1.6 M sucrose gradient containing 1 mM EDTA, 10 mM HEPES, pH 7.4. After centrifugation at 100 000 ×*g* for 20 hours in a SW40Ti rotor (Beckman), 14 fractions were collected from the bottom of the tube. For Western blot analysis, an equal volume of 20 μL of each fraction were separated on either 10% or 13% SDS-PAGE and transferred to nitrocellulose membrane. The membrane was blocked in blocking buffer (10 mM Tris-HCl, pH 7.6, 150 mM NaCl, 0.05% Tween 20) containing 5% nonfat dry milk for 2 hours at room temperature, and then, incubated with anti-NaK-ATPase (1:2500; Santa Cruz Biotechnology), anti-LAMP-1 (1:2500; BD Biosciences), anti-Rab-7 (1:2500; Santa Cruz Biotechnology), anti-EEA-1 (1:2500; Santa Cruz

Biotechnology), anti-Cytochrome C (1:2500; BD Biosciences), anti-Cx43 (1:2500; Santa Cruz Biotechnology), anti-CD38 (the M-19 antibody was raised against a 19 amino-acid sequence at C-terminal residues) (1:2500), anti-V-ATPase v0 (1:2,500; Santa Cruz Biotechnology), anti-V-ATPase v1 (1:2500; Santa Cruz Biotechnology), or anti-NMNAT3 (1:2500; Santa Cruz Biotechnology) antibodies in the blocking buffer overnight at 4°C. Blots were then washed with blocking buffer and incubated with HRP-conjugated anti-rabbit, anti-rat, anti-goat or anti-mouse antibodies (1:5000; Enzo Life Sciences) in the blocking buffer at room temperature for 2 hours. The immunoreactive proteins with respective secondary Abs were determined using an enhanced chemiluminescence kit (Amersham Pharmacia Biotech) and exposed to an LAS 4000 Image Reader Lite (Fujifilm, Japan).

2.4 | Measurement of NAADP concentration

Level of NAADP was measured using a cyclic enzymatic assay as described.[13] Briefly, samples were treated with 0.2 mL of 0.6 M perchloric acid to stop the reaction. Precipitates were removed by centrifugation at 20 000 ×*g* for 10 minutes. Perchloric acid was removed by mixing the aqueous sample with a solution containing three volumes of 2 M $KHCO_3$. After centrifugation at 15 000 ×*g* for 10 minutes, the aqueous layer was collected and neutralized with 20 mM sodium phosphate (pH 8). To remove all contaminating nucleotides, the samples were incubated with the following hydrolytic enzymes overnight at 37°C: 2.5 units/ml apyrase, 0.125 unit/mL NADase, 2 mM $MgCl_2$, 1 mM NaF, 0.1 mM PP_i, 0.16 mg/mL NMN-AT in 20 mM sodium phosphate buffer (pH 8.0). Enzymes were removed by filtration using Centricon-3 filters. After the hydrolytic treatment, alkaline phosphate (10 units/mL) was added to convert NAADP to NAAD overnight at 37°C. The alkaline phosphate was removed by filtration using Centricon-3 filters. The samples were further incubated with the cycling reagent containing 2% ethanol, 100 μg/mL alcohol dehydrogenase, 20 μM resazurin, 10 μg/mL diaphorase, 10 μM riboflavin 5′-phosphate, 10 mM nicotinamide, 0.1 mg/mL BSA, and 100 mM sodium phosphate (pH 8.0) at room temperature for 4 hours. An increase in the resorufin fluorescence was measured at 544 nm excitation and 590 nm emission using a fluorescence plate reader (Molecular Devices Corp., Spectra-Max GEMINI). Known concentrations of NAADP were used to generate a standard curve.

2.5 | Measurement of [^{3}H]NADP$^+$ transport

[^{3}H]NADP$^+$ transport was performed as described[14] with modifications. Briefly, fraction 4 was incubated with 100 μM [^{3}H]NADP and 100 μM 8-pCPT-2Me-cAMP for 30 minutes and samples were separated by a rapid oil-stop method.[15] Transported [^{3}H]NADP$^+$ was quantified by scintillation counting (PerkinElmer Life Sciences).

2.6 | Measurement of NAAD, NAD$^+$, NMN, and NAMN

NAAD, NAD$^+$, NMN, and NAMN levels were measured using liquid chromatography-tandem mass spectrometry (LC-MS/MS) as described.[16] Briefly, organelle fraction samples were diluted with HEPES buffer (20 mM HEPES pH7.4, 10 mM KCl, and 2 mM $MgCl_2$) that sucrose concentration is 0.25 M or less. Supernatant were removed by centrifugation at 15 000 ×*g* for 10 minutes. Pellet were treated with 5% of trichloroacetic acid under sonication, and precipitates were removed by centrifugation at 20 000 ×*g* for 10 minutes. Supernatants were loaded onto a Waters ACQUITY UPLC system coupled to a Waters Xevo TQ-S mass spectrometer and separated using a BEH Amide column (Waters ACQUITY UPLC BEH Amide, 130 Å, 1.7 μm, 2.1 mm × 50 mm). The column was equilibrated with 100% buffer B (90% acetonitrile/10% 50 mM ammonium formate), and eluted with a 5-minutes gradient to 60% buffer A (10 mM ammonium formate in water) at a flow rate of 0.5 mL/min. The following parameters were used for MS analysis: cone gas, 150 l/h; nebulizer, 7 Bar; and desolvation temperature, 350. The confirmation ion transitions for quantification were *m/z* 665 → 542 for NAAD, *m/z* 664 → 542.03 for NAD$^+$, *m/z* 335.06 → 123.03 for NMN, and *m/z* 336 → 124 for NAMN.

2.7 | Measurement of NADP$^+$

Level of NADP$^+$ was determined by absorbance at 340 nm of extracts by the A_2-A_1 subtractive method.[17]

2.8 | Knockdown of NMNAT1, NMNAT3, IDO, and QPRT by small interference RNA (SIRNA)

NMNAT1, NMNAT3, and scrambled siRNA were purchased from Santa Cruz Biotechnology, QPRT siRNA was purchased from ThermoFisher, and the IDO siRNA referred was as described.[18] LAK cells ^{2x105c} were cultured in an antibiotic-free growth media supplemented with fetal bovine serum. After 24 hours, LAK cells were transfected with 60 pmol of siRNA oligonucleotides specific to NMNAT1 and NMNAT3 using Lipofectamine RNAi/MAX (Invitrogen, Carlsbad, CA, USA) without antibiotics according to the instructions of the manufacturer. After 48 hours of transfection, cells were prepared for examination.

2.9 | Reverse transcription polymerase chain reaction (RT-PCR)

Total RNA was isolated from LAK cells using the Hybrid-R Kit (GeneAll). cDNA was synthesized by reverse transcription from 1 μg total RNA using a ImProm-II Reverse Transcription System (Promega). Primers for NMNAT1, NMNAT2, NMNAT3, and GAPDH were 5′-TGCCCAACT TGTGGAAGATG-3′ (NMNAT1 forward primer), 5′- AAT GGTTGTGCTTGGCCTCT-3′ (NMNAT1 reverse primer), 5′- TGGAGCGCTTCACTTTTGTAG-3′ (NMNAT2 forward primer), 5′- GATGTACAGCTGACTCTTGA-3′ (NMNAT2 reverse primer), 5′- AGCACTGCCAGAGTTGAAAC-3′ (NMNAT3 forward primer), 5′- CTTTCCAGGAACCGTCA TTG-3′ (NMNAT3 reverse primer), 5′-CGTGGAGTCTAC TGGTGTCTT-3′ (GAPDH forward primer) and 5′-GTTGG TGGTGCAGGATGCATT-3′ (GAPDH reverse primer). Thirty cycles of amplification were carried out as follows: 30 seconds at 94°C; 30 seconds at 62°C; 30 seconds at 72°C, followed by 5 minutes elongation at 72°C.

2.10 | NAADP transport

NAADP transport experiments were performed as described[14] with minor modifications. Briefly, Fraction 4 was incubated with inhibitors and 100 μM 8-pCPT-2Me-cAMP for 30 minutes at 37°C and the reaction mixes were separated by rapid oil-stop.[15] NAADP was measured by a cyclic enzymatic assay.

2.11 | Immunoprecipitation

Organelle fraction 4 was incubated 100 μM 8-pCTP-2Me-cAMP for 30 minutes at 37°C, and then, lysed with an ice-cold lysis buffer (20 mM Tris-HCl, pH 7.2, 2% NP-40, 150 mM NaCl, 1 mM phenylmethylsulfonyl fluoride (PMSF), 10 μg/mL leupeptin, 10 μg/mL pepstatin, and 10 μg/mL aprotinin). After centrifugation at 20 000 ×*g* for 10 minutes, supernatants were taken. For immunoprecipitation, lysate precleared with protein G-agarose was incubated with anti-CD38 mAb (clone 90; eBioscience) overnight at 4°C, and then, further incubated with protein G-agarose at 4°C for 1 hours. The immunoprecipitates were washed four times with lysis buffer, and then, used for western blot and HPLC.

2.12 | Cell migration assay by agarose spot assay

Chemokine-induced cell migration assay was performed as described.[19] About 0.1 g of low-melting point agarose (Invitrogen) was placed into a 100 mL beaker and diluted into 20 mL PBS to make a 0.5% of agarose solution. This was heated on a hot plate in the cell culture hood until boiling, swirled to facilitate complete dissolution, and then, taken off of the heat. When the temperature cooled to 40°C, 90 μL of agarose solution was pipetted into a 1.5-mL Eppendorf tube containing 10 μL of PBS with or without IL8 (Sigma). Ten-microliter spots of agarose containing IL8 were pipetted, using cut pipet tips (Cat. no. 70.760.211; Sarstedt, Leicester, UK), as rapidly as possible onto 35-mm glass-bottomed dishes (SPL, Korea), and allowed to cool for ~5 minutes at 4°C. Four spots per dish were pipetted, two containing IL8 and two containing only PBS. At this point cells were plated into spot-containing dishes in the presence of 10% of FBS cell culture media and allowed to adhere for 4 hours. Cells were transferred into cell culture media or Hanks' balanced salt solution (Invitrogen) with 10 mM HEPES (Sigma-Aldrich, Dorset, UK) for time-lapse studies with 0.1% of FBS, replaced into the incubator for 4 hours, and analyzed by microscopy. Imaging was performed on a Nikon TE300 inverted microscope with a 10× objective (Nikon, Surrey, UK), and for each spot, we recorded the field that contained the highest apparent number of motile cells penetrating furthest underneath the agarose spot.

2.13 | High pressure liquid chromatography (HPLC)

NAADP was quantified as described.[20] Nucleotide synthesis reactions from $NADP^+$ and NAAD substrates contained 20 mM sodium acetate (pH 4.5), 1 mM calcium chloride, 1 mM magnesium chloride. For HPLC analysis, nucleotides were separated on a column (3 × 150 mm), packed with AGMP-1 resin (Bio-Rad Laboratories). Samples (100 μL) were injected onto a column equilibrated with water. The bound material was eluted with a concave-up gradient of trifluoroacetic acid, which increased linearly to 2% at 1.5 minutes and to 4, 8, 16, 32, and 100% (150 mM trifluoroacetic acid) at 3, 4.5, 6.0, 7.5, and 7.51 minutes, respectively. The flow rate was 4 mL/minutes. Nucleotides were detected by an absorbance at 254 nm. Detection of NAMN, NAD^+, NAAD was performed by reverse phase HPLC method as described.[21] Nucleotides were separated on a BDS hyperseal C18 column (Thermo). Samples (100 μL) were injected onto a column equilibrated with 0.05 M phosphates buffer. The HPLC is run at a flow rate of 1 mL/min with 100% buffer A (0.05 M Phosphate Buffer) from 0 to 5 minutes, a linear gradient to 95% buffer A/5% buffer B (100% of methanol) from 5 to 6 minutes, 95% buffer A/5% buffer B from 6 to 11 minutes, a linear gradient to 85% buffer A/15% buffer B from 11 to 13 minutes, 85% buffer A/15% buffer B from 13 to 23 minutes, a linear gradient to 100% buffer A from 23 to 24 minutes, and 100% buffer A from 24 to 30 minutes.

The flow rate was 1 mL/min. Nucleotides were detected by absorbance at 261 nM.

2.14 | Quantification and statistical analysis

Data are expressed as means ± SEM. Statistical comparisons were performed with analysis of variance (ANOVA) using Sigma plot. Significant differences between groups were determined with the unpaired Student's *t* test. Statistical significance was set at $P < .05$.

3 | RESULTS

3.1 | NAADP is produced in endolysosome-containing fractions by using the substrate NAAD as the NA donor

We have previously shown that in LAK cells, binding of IL8 to CXCR1 leads to activation of guanylyl cyclase and PKG, which leads to internalization of CD38 and cADPR production.[9,10] In turn, cADPR-mediated Ca^{2+} release induces NAADP production in lysosome-related acidic organelles, resulting in IL8-driven cell migration in a manner that depends on EPAC, protein kinase A, and RAP1.[12] To identify the organelles that mediate production of NAADP, we treated LAK cells with IL8 and measured metabolite and protein levels in each subcellular fraction. Though CD38 was present in all fractions, only fraction 4 showed IL8-dependent production of NAADP. Fraction 4 was positive for late endosomal and lysosomal markers, Rab 7, and LAMP1 (Figure 1). Notably, fraction 4 contains not only 42 kDa type II CD38, but also 36 kDa type III CD38, suggesting that CD38 exists in type II and III forms with opposing membrane orientations.

To determine the substrates for signal-dependent NAADP production, we quantified levels of NAD^+ metabolites[22] in fractions before and after IL8 stimulation. Liquid-chromatography tandem mass spectrometry analysis revealed significantly decreased nicotinic acid adenine dinucleotide (NAAD) levels and increased NAD^+ levels in fraction 4 after IL8 treatment (Supplemental Figure S1A,B) while levels of nicotinic acid mononucleotide (NAMN), nicotinamide mononucleotide (NMN), and $NADP^+$ (Supplemental Figure S1C-E) remained unchanged. These findings suggest that NAAD might serve as the NA donor for formation of NAADP.

3.2 | Endolysosomal naadp production depends on cytosolic $nadp^+$ transported by Cx43

Because EPAC is an obligate mediator of NAADP formation in IL8-treated LAK cells,[12] we tested whether NAADP formation increased when fraction 4 was treated with 8-pCPT-2′-O-Me-cAMP, a cAMP analog, and selective EPAC activator. The activator increased NAADP formation in fraction 4 only when cytosol was provided (Figure 2A), suggesting that import of an EPAC-dependent cytosolic component may be needed for NAADP synthesis. Given that $NADP^+$ is an in

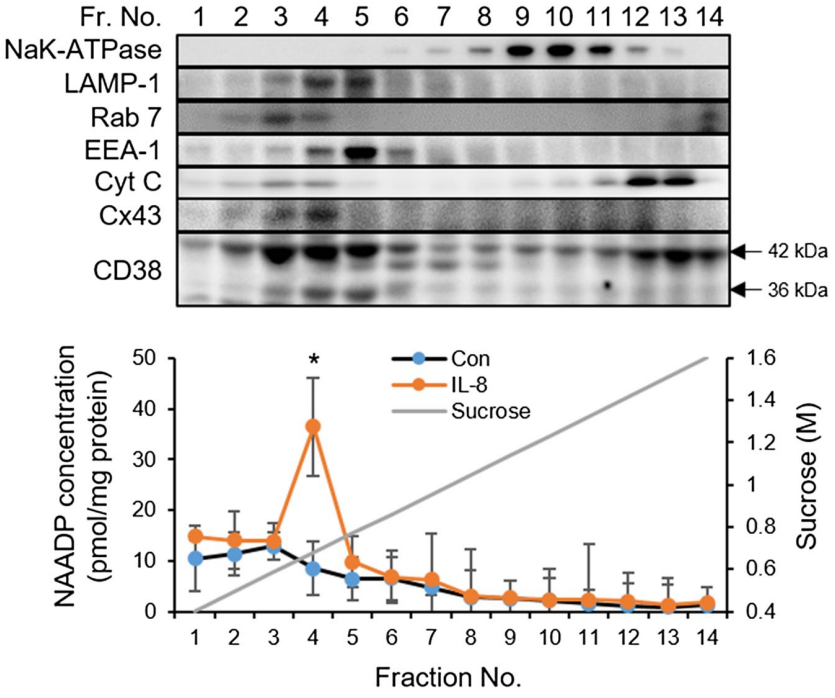

FIGURE 1 IL8 dependent NAADP formation occurs in a Rab 7 and LAMP-1 rich subcellular compartment. Subcellular fractionation of IL8-treated LAK cells identifies a unique CD38-containing fraction where NAADP is formed. CD38 was detected using an anti-CD38 M-19 antibody as described in the Materials and Methods. Arrows indicate type II and type III CD38. Mean ± SEM of three independent experiments is shown. *$P < .05$, control versus IL8

vitro substrate for NAADP formation,[3,4] we tested whether $NADP^+$ might substitute for cytosol in IL8-dependent NAADP formation by fraction 4. Moreover, because we identified high levels of Cx43, a known NAD^+ transporter,[23] in fraction 4 (Figure 1), we tested whether the EPAC-dependent cytosol requirement might be blocked by the Cx43 inhibitor, oleamide. As shown in Figure 2A, $NADP^+$ can substitute for cytosol in 8-pCPT-2′-O-Me-cAMP-stimulated NAADP formation in a manner that is sensitive to oleamide. In support of the Cx43 transport mechanism for EPAC-dependent NAADP formation, we showed that [^{3}H]-$NADP^+$ transport into fraction 4 is stimulated by the cAMP analog and blocked by the Cx43 inhibitor (Figure 2B). Thus, IL8 and cAMP signaling drive a CD38 substrate into endolysosomes for NAADP formation.

3.3 | Endolysosomal NAADP synthesis is catalyzed by type II CD38 utilizing NAAD and $NADP^+$

The ability of CD38 to form NAADP rather than cADPR or ADPR depends on acidic pH.[3,4,13] It has been established that endolysosomal acidification depends on assembly of the V_1 and V_0 subunits of V-ATPase.[24] We discovered that fraction 4 contains V_0 but not V_1 subunits until cells are stimulated by IL8 (Supplemental Figure S2). Moreover, as shown in Figure 2A, bafilomycin A1, an inhibitor of V-ATPase, completely blocked EPAC activator-induced NAADP synthesis. The requirement for organelle acidification and the involvement of Cx43-dependent $NADP^+$ transport suggested that type II CD38, whose catalytic domain is in the lumen

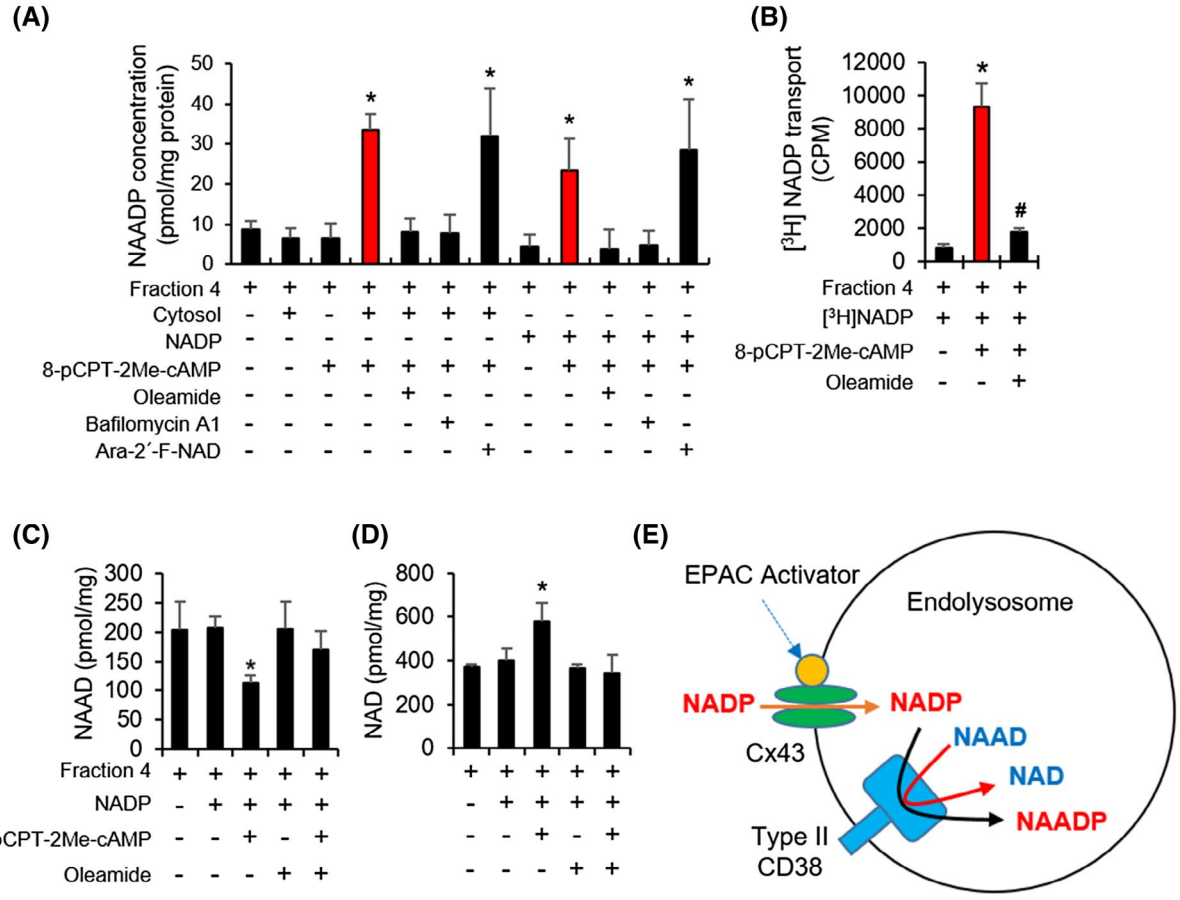

FIGURE 2 Signal-dependent NAADP formation depends on endolysosomal acidification, type II CD38 and Epac-dependent import of $NADP^+$. A, Reconstituted NAADP formation from IL8-stimulated LAK cells occurs in a compartment that is acidified in a bafilomycin-inhibitable manner with cytosol that can be substituted by $NADP^+$, which is transported in an EPAC- and Cx43-dependent fashion. NAADP synthesis was measured in fraction 4 after incubation with cytosol (60 μg) or $NADP^+$ (100 μM) in presence or absence of EPAC activator, 8-pCPT-2Me-cAMP for 30 min at 37°C. EPAC activator-induced NAADP synthesis was blocked by 100 μM oleamide (Cx43 inhibitor) and 1 μM bafilomycin A1 (lysosomal V-type H^+-ATPase inhibitor) but not by 200 nM ara-2′-F-NAD^+, a membrane-impermeable CD38 inhibitor. B, $NADP^+$ (100 μM) is transported (30 minutes, 37°C) into Cx43-rich endolysosomes in a manner that depends upon EPAC stimulation (100 μM 8-pCPT-2Me-cAMP) and blocked by Cx43 inhibition (100 μM oleamide). C,D, EPAC-stimulated NAADP formation is accompanied by stoichiometric depression of NAAD and formation of NAD^+ quantified by LC-MS/MS E, Schematic of NAADP formation in endolysosomes. Mean ± SEM of three independent experiments, *effect of $NADP^+$ and EPAC activator, and #effect of oleamide, $P < .05$

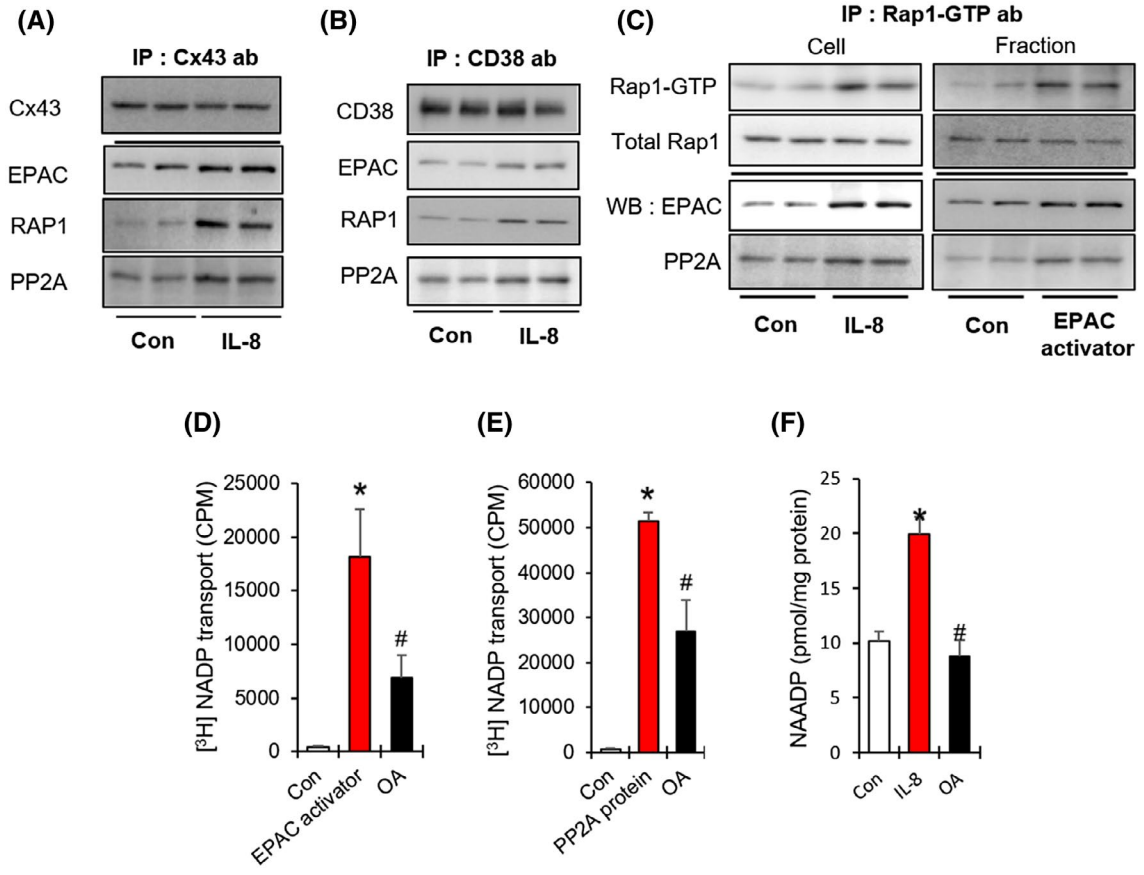

FIGURE 3 EPAC-RAP1-PP2A mediate $NADP^+$ transport via Cx43 dephosphorylation. A, IL8 induces association of EPAC-RAP1-PP2A complex with Cx43. B, IL8 induces association of EPAC-RAP1-PP2A complex with CD38. C, IL8 and EPAC activator increase association of RAP1-GTP with EPAC-PP2A in LAK cells and endolysosome fraction. D, OA inhibits EPAC activator-induced $NADP^+$ transport to endolysosome fraction. E, OA inhibits PP2A-induced $NADP^+$ transport to the endolysosome fraction. F, OA inhibits IL8-induced NAADP formation. Mean ± SEM of three independent experiments is shown. $^*P < .05$, control versus EPAC activator; $^{\#}P < .05$, EPAC activator versus OA

of organelles,[10] must be responsible for NAADP production. We confirmed this by showing that ara-2′-F-NAD^+, a membrane-impermeable CD38 inhibitor, is incapable of blocking EPAC activator-induced NAADP synthesis by fraction 4 (Figure 2A).

Given that cellular NAAD levels were depressed by IL8 treatment (Supplemental Figure S1), we further analyzed NAD^+ metabolite levels in fraction 4 in the presence of $NADP^+$ before and after EPAC activator treatment. As in the reconstitution experiments with IL8-induced cell lysates (Figure 1), NAAD levels were significantly depressed and NAD^+ levels were significantly increased after treating fraction 4 with the EPAC activator and $NADP^+$ (Figure 2C,D), with NAMN and NMN levels remaining unaltered (Supplemental Figure S3). Changes in NAAD and NAD^+ levels were blocked by oleamide (Figure 2C,D). To exclude the possibility that NAAD was being converted to NAD^+ by glutamine-dependent NAD^+ synthetase,[25] we reconstituted the proposed reaction (NAAD + $NADP^+$ NAADP + NAD^+, Figure 2E) with purified CD38 (Supplemental Figure S4). This reaction required only NAAD plus $NADP^+$ under acidic conditions, produced stoichiometric amounts of NAADP and NAD^+, and exhibited no requirement for glutamine or ATP.

3.4 | EPAC-RAP1-PP2A mediate $NADP^+$ transport via Cx43 dephosphorylation

A signal-dependent mechanism for NAADP formation must gate $NADP^+$ import into an acidified CD38-containing organelle with high temporal specificity. Protein phosphatase PP2A is known to dephosphorylate Cx43.[26] Additionally, PP2A activity is positively modulated by cAMP in an EPAC and RAP1-dependent manner.[27] Thus, we tested whether EPAC-RAP1-PP2A signaling might drive Cx43-mediated $NADP^+$ transport. We discovered that IL8 stimulation increases association of EPAC, RAP1, and PP2A proteins with Cx43 (Figure 3A) and CD38 (Figure 3B). In whole cell extracts and fraction 4, both IL8 and EPAC activator increased the proportion of RAP1 in the GTP-bound form and its association with EPAC and PP2A

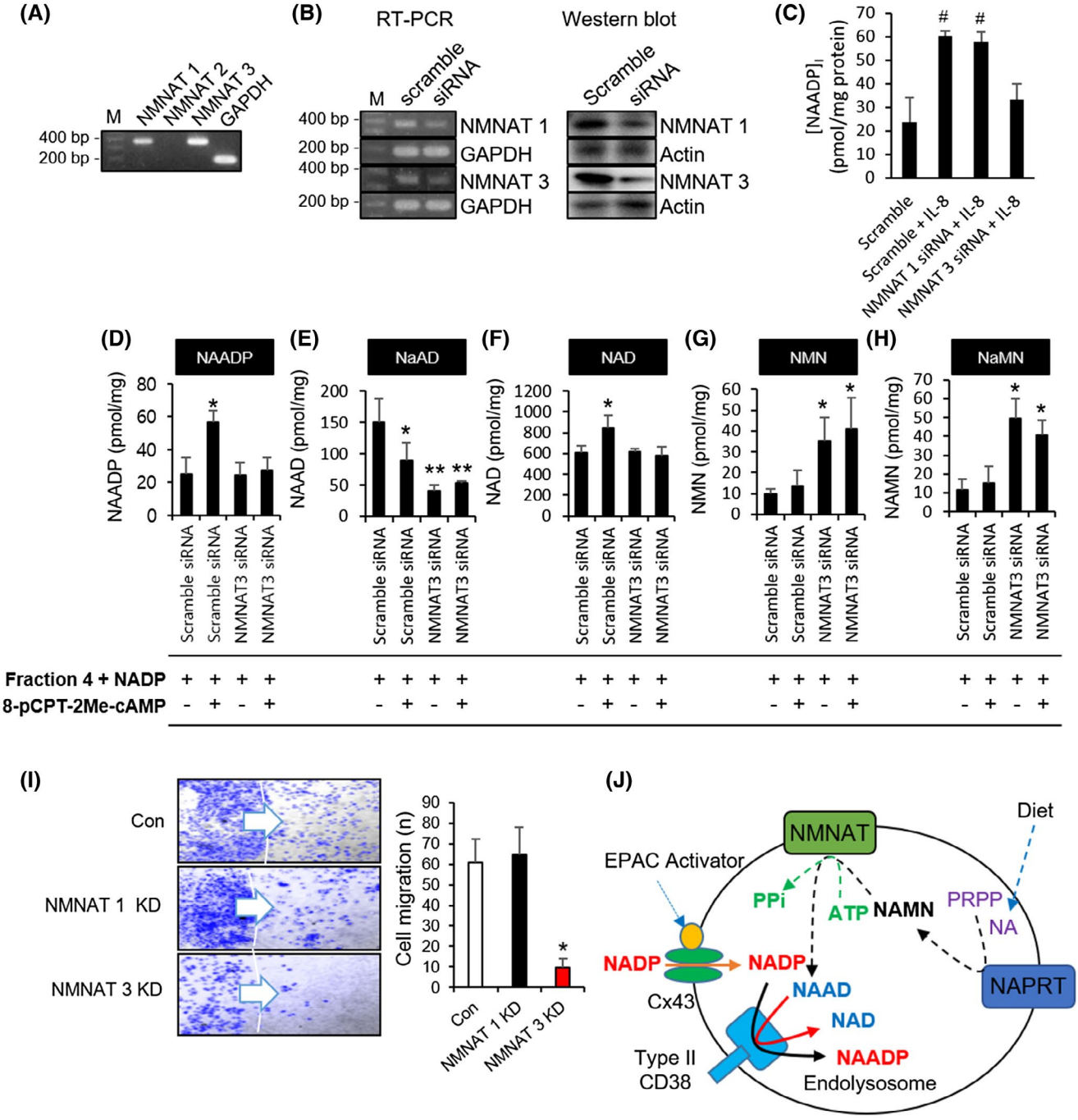

FIGURE 4 NMNAT3 is required to produce endolysosomal NAAD to effect IL8-driven NAADP-mediated chemotaxis. A, B, mRNA expression of NMNAT1-3 in LAK cells as modulated by siRNA treatment and as assessed by Western blot. C, IL8-induced NAADP formation in LAK cells is dependent on NMNAT3. D-H, EPAC activator-induced NAADP formation in LAK cells depends on NMNAT3. $NADP^+$ and EPAC activator-dependent nucleotide levels in fraction 4 depend on specific NMNAT isozymes. Endolysosomal concentrations of NAAD, NAD^+, NMN, and NAMN were determined by LC-MS after incubation (30 minutes at 37°C) with 100 μM $NADP^+$ plus or minus 8-pCPT-2Me-cAMP as a function of NMNAT3 status (E-H*)*. The data indicate that NMNAT3 is required for NAAD formation and nonaccumulation of both NAMN and NAD^+. Upon EPAC stimulation, CD38 converts $NADP^+$ and NAAD to NAADP plus NAD^+. I, IL8-induced chemotaxis of LAK cells is sensitive to NMNAT3 knockdown (KD). J, Schematic of formation of NAAD via NAPRT and NMNAT3 in endolysosomes. Mean ± SEM of three independent experiments. $^{\#}P < .05$ versus IL8 treated LAK cells; $^{*}P < .05$, versus fraction 4 of scramble siRNA with 8-pCPT-2Me-cAMP; $^{**}P < .05$ versus fraction 4 of NMNAT 3 siRNA

(Figure 3C). Moreover, we found that both IL8 and the EPAC activator increased dephosphorylation of Cx43 at Ser-279 (Supplemental Figure S5), suggesting that Cx43 dephosphorylation by PP2A induces $NADP^+$ transport into endolysosomes. We further found that treatment with the PP2A inhibitor okadaic acid (OA) blocks the transport of

$NADP^+$ into fraction 4 organelles, induced by either an Epac activator (Figure 3D) or purified PP2A (Figure 3E). These findings indicate that PP2A, once activated by EPAC and RAP1, dephosphorylates and gates Cx43 for $NADP^+$, enabling production of NAADP by CD38 in endolysosomes upon IL8 treatment (Figure 3F).

3.5 | NMNAT3 and NAPRT are required to produce endolysosomal NAAD to effect IL8-driven NAADP-mediated chemotaxis

Because $NADP^+$ was identified as the only cytosolic NAD^+ metabolite required to stimulate IL-8 or EPAC-signaled NAADP formation, and we identified NAAD as present in fraction 4 (Supplemental Figure S1A and Figure 2C), we surmised that an NAMN adenylyltransferase activity must be localized in this fraction in order to produce the NAAD substrate. Three isoforms of NAMN/NMN adenyltransferase (NMNAT) are encoded by vertebrates.[28] RT-PCR data showed that LAK cells express NMNAT1 and NMNAT3 (Figure 4A). NMNAT1 and NMNAT3 have been termed the nuclear and mitochondrial isoforms, respectively,[28] though the null phenotype in mice is not consistent with this assignment for NMNAT3.[29] We used siRNAs to knock down NMNAT1 and NMNAT3 at the level of mRNA and protein (Figure 4B). We discovered that IL8-induced NAADP formation in LAK cells was abolished by NMNAT3 knockdown but was unaffected by NMNAT1 knockdown (Figure 4C). Similarly, EPAC activator-induced NAADP formation in fraction 4 depended on NMNAT3 but not NMNAT1 (Figure 4D and Supplemental Figure S6A). We further showed that fraction 4 contained high levels of NMNAT3 (Supplemental Figure S2). To further establish that NMNAT3 is responsible for NAAD synthesis in endolysosomes, we quantified levels of NAD^+ metabolites in fraction 4 from LAK cells as a function of additions of EPAC activator and/or $NADP^+$ and knockdown of NMNAT1 or NMNAT3. As expected, NAAD and NAD^+ levels were significantly lower in samples from NMNAT3 knockdown cells when compared with those taken from NMNAT1 knockdown cells or control cells (Figure 4E,F and Supplemental Figure S6B,C). Consistent with known biosynthetic pathways,[11] NAMN and NMN levels were significantly higher in the NMNAT3 and NMNAT1 knockdown LAK cells when compared to control cells (Figure 4G,H and Supplemental Figure S6D,E). Gallotannin has been characterized as an inhibitor of NMNAT with strong activity against the NMNAT3 isoform.[28] We therefore examined the effect of gallotannin on EPAC activator-induced NAADP synthesis in fraction 4. Consistent with the hypothesis that an endolysosomal NMNAT3 activity is required to produce the NAAD substrate for NAADP synthesis, we found that gallotannin blocked EPAC activator-induced NAADP synthesis, resulting in significantly lower levels of NAAD and NAD^+ and higher levels of NAMN and NMN in lysed fractions (Supplemental Figure S6F-J).

Having established that the CD38 substrate NAAD is produced by endolysosomal NMNAT3, we asked how the NMNAT substrate, NAMN, is synthesized. NAMN is synthesized either by de novo biosynthetic enzymes or by salvage of nicotinic acid,[11] As shown in Supplemental Figure S7A, knockdown of the first and last de novo enzymes indoleamine 2,3 dioxygenase (IDO) and quinolinic acid phosphoribosyltransferase (QPRT) reduced IL8-induced NAMN abundance in fraction 4. In addition, the nicotinic acid salvage enzyme NA phosphoribosyltransferase (NAPRT)[30] is abundant in fraction 4 (Supplemental Figure S7B) and NAAD synthesis was reconstituted from immunoprecipitated NAPRT from fraction 4 in a reaction with NA, PRPP, ATP, and recombinant NMNAT (Supplemental Figure S7C).

Collectively these data establish that endolysosomes contain both the de novo and NA salvage enzymes for synthesis of one CD38 substrate, NAAD, the signal-dependent import machinery for the other substrate, $NADP^+$, and a signal-dependent compartment acidification mechanism for NAADP formation from $NADP^+$ and NAAD for type II CD38 activity. Earlier, it was shown that LAK cells from CD38 knockout mice cannot be induced to migrate by IL8 treatment.[12] To test whether the proposed NAADP synthesis pathway is functionally important, we treated control, NMNAT1 and NMNAT3 knockdown cells with IL8 and assayed cell migration. As shown in Figure 4I, though both of these treatments depress total cellular NAAD and NAD^+, only the NMNAT3 knockdown depressed cellular migration.

4 | DISCUSSION

In the current study, we discovered how cellular signaling directs substrates into endolysosomes for NAADP production. CD38 has been characterized as a type II and type III plasma membrane protein with its active site either extracellular (type II) or cytosolic (type III). However, here, we showed that CD38 is abundant in endolysosomes in LAK cells (Figure 1) with a type II orientation that places the catalytic domain in the lumen of this organelle. This explains several previously mysterious aspects of NAADP formation. First, it has long been appreciated that CD38-mediated base-exchange reaction requires an acidic environment but it was not known how this occurs.[12] Here, we show that this is achieved by a signal-dependent organelle acidification mechanism (Supplemental Figure S2). Second, type II CD38 is constitutively active, which would demand limited access to a substrate for regulation of NAADP production. Our findings show that there is signal-dependent import of $NADP^+$ into endolysosomes (Figure 2). We also resolved the long-time mystery of what

the NA donor is. As a bona fide substrate for the base-exchange reaction for NAADP synthesis, NAAD was found to be synthesized by both de novo and NA salvage enzymes in endolysosomes (Supplemental Figure S7).

Previously, we demonstrated that cADPR formation is mediated specifically by type III CD38 in early endosomes. However, in this case, the catalytic domain faces the cytosol, where CD38 utilizes NAD^+ in a cyclization reaction that produces cADPR at neutral pH.[31] These findings indicate that CD38-mediated synthesis of cADPR and NAADP is operated by different pools of CD38 with opposite orientation, located in different organelles.[12] Given that cADPR formation precedes NAADP formation in LAK cells in response to IL8, this mode of biogenesis of Ca^{2+}-mobilizing messengers may determine key features of signal-specific spatiotemporal Ca^{2+} signaling. In the case of IL8-induced LAK cells, the sequential production of IP_3, cADPR and NAADP may be required for cellular chemotaxis (Figure 5).

Consistent with previous findings in the sea urchin egg and mammalian cells that cADPR and NAADP production are differentially regulated by cGMP and cAMP, respectively,[12,32] the signal-dependent organization of machineries for NAADP production were strictly cAMP-dependent. This includes the assembly of V_1 and V_0 subunits of V-ATPase for endolysosomal acidification and activation of Cx43 to transport $NADP^+$ into the lumen of endolysosomes. These data strongly suggest that the described mechanism of NAADP formation is conserved in a wide range of species.

Previous work[33] has shown that CD38-mediated chemotaxis via IL8 is characterized by the proteolytic cleavage of CD38 in human neutrophils; the addition of IL8 to neutrophils resulted in decreased CD38 expression, paralleled by its accumulation in the supernatant. The addition of a p38 MAP kinase inhibitor or a serine protease inhibitor blocked the IL8-induced decrease of CD38 in neutrophils as well as its increase in supernatants. These findings suggest that the proteolytic cleavage of CD38 is somehow involved in CD38-mediated chemotaxis in human neutrophils in response to IL8. However, these findings were observed 2 hours after IL8 stimulation, which is in contrast to the time point seen in IL8-driven endolysosomal activity 1-2 minutes after IL8 stimulation. Although we do not know how the two signaling events are interrelated in terms of IL8-induced chemotaxis, CD38-mediated Ca^{2+} signaling events occur very acutely in cellular organelles after IL8 stimulation, while the proteolytic cleavage of CD38 is likely an independent and later result of IL8-induced chemotaxis.

We used a model cell system to dissect how a Ca^{2+}-mobilizing messenger NAADP plays a role for chemokine-dependent cell migration. Intriguingly, EPAC, RAP1, Cx43, and V-ATPase, all of which are essential for NAADP production, have been found to be involved in cell migration as well as cancer metastasis through unknown mechanisms.[34-38] Thus, we suggest that endolysosomal NAADP synthesis by type II CD38 integrates cell surface inputs through these membrane-associated proteins to effect Ca^{2+}-dependent cell migration. Moreover, targeting of Ca^{2+}-dependent cell migration could offer a strategy for the development of therapeutics against cancer metastasis.

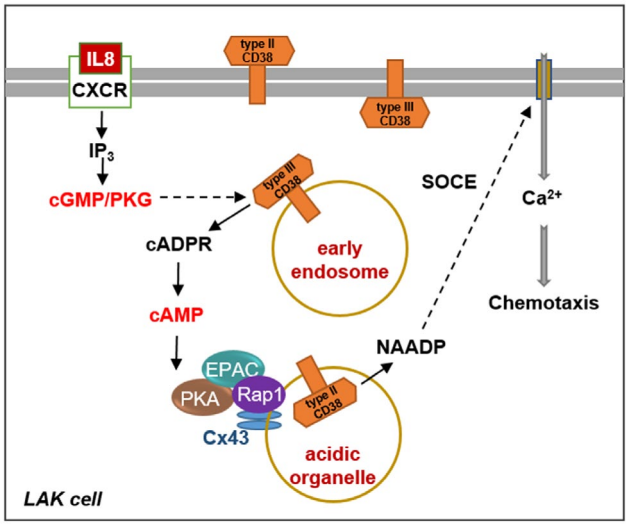

FIGURE 5 Schematic diagram of the IL8-induced signaling pathway in LAK cells. IL8 receptor (CXCR) ligation stimulates phospholipase C (PLC), resulting in the production of IP_3. IP_3 binds to the receptor, releasing Ca^{2+} from ER Ca^{2+} stores. The IP_3-mediated increase in intracellular Ca^{2+} levels results in increased cGMP levels via guanylyl cyclase, thus, activating PKG. CD38 is internalized into early endosomes (EE) in a PKG-dependent manner, resulting in cADPR production. cADPR-mediated Ca^{2+} release via the ryanodine receptor (RYR) increases cAMP levels via adenylyl cyclase, activating PKA and EPAC. PKA/EPAC then activates Rap1, which induces NAADP production inside acidic organelles. NAADP-mediated Ca^{2+} release ultimately occurs through Ca^{2+} influx from store-operated Ca^{2+} entry (SOCE), resulting in LAK cell chemotaxis

ACKNOWLEDGMENTS

We thank Dr Chansu Park for critical reading of the manuscript. This work was supported by Korean National Research Foundation Grant 2012R1A3A2026453 to UHK, 2014R1A6A1030318 to HTC, and funds from the Roy J. Carver Trust to CB CB owns stock in ChromaDex and serves as their chief scientific advisor. He also serves on the scientific advisory board of Cytokinetics.

CONFLICT OF INTEREST

The authors declare no competing interests.

AUTHOR CONTRIBUTIONS

U. H. Kim designed research; T. S. Nam and D. R. Park performed research with help from S. Y. Rah and T. G. Woo; U.

H. Kim, H. T. Chung, T. S. Nam, D. R. Park, and C. Brenner analyzed data; U. H. Kim and C. Brenner wrote the paper with help from T. S. Nam, D. R. Park, and H. T. Chung.

REFERENCES

1. Lee HC, Aarhus R, Graeff RM. Sensitization of calcium-induced calcium release by cyclic ADP-ribose and calmodulin. *J Biol Chem*. 1995;270:9060-9066.
2. Churchill GC, Okada Y, Thomas JM, Genazzani AA, Patel S, Galione A. NAADP mobilizes Ca^{2+} from reserve granules, lysosome-related organelles, in sea urchin eggs. *Cell*. 2002;111:703-708.
3. Aarhus R, Graeff RM, Dickey DM, Walseth TF, Lee HC. ADP-ribosyl cyclase and CD38 catalyze the synthesis of a calcium-mobilizing metabolite from NADP. *J Biol Chem*. 1995;270:30327-30333.
4. Graeff RM, Franco L, De Flora A, Lee HC. Cyclic GMP-dependent and -independent effects on the synthesis of the calcium messengers cyclic ADP-ribose and nicotinic acid adenine dinucleotide phosphate. *J Biol Chem*. 1998;273:118-125.
5. Cancela JM, Churchill GC, Galione A. Coordination of agonist-induced Ca^{2+}-signalling patterns by NAADP in pancreatic acinar cells. *Nature*. 1999;398:74-76.
6. Churchill GC, O'Neill JS, Masgrau R, et al. Sperm deliver a new second messenger: NAADP. *Curr Biol*. 2003;13:125-128.
7. Guse AH, Lee HC. NAADP: a universal Ca^{2+} trigger. *Sci Signal*. 2008;1:re10.
8. Zhao YJ, Lam CM, Lee HC. The membrane-bound enzyme CD38 exists in two opposing orientations. *Sci Signal*. 2012;5:ra67.
9. Rah SY, Park KH, Han MK, Im MJ, Kim UH. Activation of CD38 by interleukin-8 signaling regulates intracellular Ca^{2+} level and motility of lymphokine-activated killer cells. *J Biol Chem*. 2005;280:2888-2895.
10. Rah SY, Kim UH. CD38-mediated Ca^{2+} signaling contributes to glucagon-induced hepatic gluconeogenesis. *Sci Rep*. 2015;5:10741.
11. Bogan KL, Brenner C. Nicotinic acid, nicotinamide, and nicotinamide riboside: a molecular evaluation of NAD^+ precursor vitamins in human nutrition. *Annu Rev Nutr*. 2008;28:115-130.
12. Rah SY, Mushtaq M, Nam TS, Kim SH, Kim UH. Generation of cyclic ADP-ribose and nicotinic acid adenine dinucleotide phosphate by CD38 for Ca^{2+} signaling in interleukin-8-treated lymphokine-activated killer cells. *J Biol Chem*. 2010;285:21877-21887.
13. Graeff R, Lee HC. A novel cycling assay for nicotinic acid-adenine dinucleotide phosphate with nanomolar sensitivity. *Biochem J*. 2002;367:163-168.
14. Park KH, Kim BJ, Shawl AI, Han MK, Lee HC, Kim UH. Autocrine/paracrine function of nicotinic acid adenine dinucleotide phosphate (NAADP) for glucose homeostasis in pancreatic β-cells and adipocytes. *J Biol Chem*. 2013;288:35548-35558.
15. Kim UH, Han MK, Park BH, Kim HR, An NH. Function of NAD glycohydrolase in ADP-ribose uptake from NAD by human erythrocytes. *Biochim Biophys Acta*. 1993;1178:121-126.
16. Tong L, Lee S, Denu JM. Hydrolase regulates NAD^+ metabolites and modulates cellular redox. *J Biol Chem*. 2009;284:11256-11266.
17. Zhang Z, Yu J, Stanton RC. A method for determination of pyridine nucleotides using a single extract. *Anal Biochem*. 2000;285:163-167.
18. Yen MC, Lin CC, Chen YL, et al. A novel cancer therapy by skin delivery of indoleamine 2,3-dioxygenase siRNA. *Clin Cancer Res*. 2009;15:641-649.
19. Wiggins H, Rappoport J. An agarose spot assay for chemotactic invasion. *Biotechniques*. 2010;48:121-124.
20. Vasudevan SR, Galione A, Churchill GC. Sperm express a Ca^{2+}-regulated NAADP synthase. *Biochem J*. 2008;411:63-70.
21. Yoshino J, Imai S. Accurate measurement of nicotinamide adenine dinucleotide (NAD^+) with high-performance liquid chromatography. *Methods Mol Biol*. 2013;1077:203-215.
22. Trammell SA, Brenner C. Targeted, LCMS-based metabolomics for quantitative measurement of NAD^+ metabolites. *Comput Struct Biotechnol J*. 2013;4:e201301012.
23. Bruzzone S, Guida L, Zocchi E, Franco L, De Flora A. Connexin 43 hemi channels mediate Ca^{2+}-regulated transmembrane NAD^+ fluxes in intact cells. *FASEB J*. 2001;15:10-12.
24. Xu Y, Parmar A, Roux E, et al. Epidermal growth factor-induced vacuolar (H^+)-atpase assembly: a role in signaling via mTORC1 activation. *J Biol Chem*. 2012;287:26409-26422.
25. Bieganowski P, Pace HC, Brenner C. Eukaryotic NAD^+ synthetase Qns1 contains an essential, obligate intramolecular thiol glutamine amidotransferase domain related to nitrilase. *J Biol Chem*. 2003;278:33049-33055.
26. Ai X, Pogwizd SM. Connexin 43 downregulation and dephosphorylation in nonischemic heart failure is associated with enhanced colocalized protein phosphatase type 2A. *Circ Res*. 2005;96:54-63.
27. Hong K, Lou L, Gupta S, Ribeiro-Neto F, Altschuler DL. A novel Epac-Rap-PP2A signaling module controls cAMP-dependent Akt regulation. *J Biol Chem*. 2008;283:23129-23138.
28. Berger F, Lau C, Dahlmann M, Ziegler M. Subcellular compartmentation and differential catalytic properties of the three human nicotinamide mononucleotide adenylyltransferase isoforms. *J Biol Chem*. 2005;280:36334-36341.
29. Yamamoto M, Hikosaka K, Mahmood A, et al. Nmnat3 Is dispensable in mitochondrial NAD level maintenance in vivo. *PLoS One*. 2016;11:e0147037.
30. Hara N, Yamada K, Shibata T, Osago H, Hashimoto T, Tsuchiya M. Elevation of cellular NAD levels by nicotinic acid and involvement of nicotinic acid phosphoribosyltransferase in human cells. *J Biol Chem*. 2007;282:24574-24582.
31. Park DR, Nam TS, Kim YW, Bae YS, Kim UH. Oxidative activation of type III CD38 by NADPH oxidase-derived hydrogen peroxide in Ca^{2+} signaling. *FASEB J*. 2019;33:3404-3419.
32. Wilson HL, Galione A. Differential regulation of nicotinic acid-adenine dinucleotide phosphate and cADP-ribose production by cAMP and cGMP. *Biochem. J*. 1998;331:837-843.
33. Fujita T, Zawawia KH, Kuriharab H, Van Dyke TE. CD38 cleavage in fMLP- and IL-8-induced chemotaxis is dependent on p38 MAP kinase but independent of p44/42 MAP kinase. *Cell Signal*. 2005;17:167-175.
34. Almahariq M, Tsalkova T, Mei FC, et al. A novel EPAC-specific inhibitor suppresses pancreatic cancer cell migration and invasion. *Mol Pharmacol*. 2013;83:122-128.
35. Kato Y, Yokoyama U, Yanai C, et al. Epac1 deficiency attenuated vascular smooth muscle cell migration and neointimal formation. *Arterioscler Thromb Vasc Biol*. 2015;35:2617-2625.

36. Lorraine C, Wright CS, Martin PE. Connexin43 plays diverse roles in co-ordinating cell migration and wound closure events. *Biochem Soc Trans*. 2015;43:482-488.
37. Ring S, Pushkarevskaya A, Schild H, et al. Regulatory T cell-derived adenosine induces dendritic cell migration through the Epac-Rap1 pathway. *J Immunol*. 2015;194:3735-3744.
38. Stransky L, Cotter K, Forgac M. The function of V-ATPases in cancer. *Physiol Rev*. 2016;96:1071-1091.

SUPPORTING INFORMATION

Additional Supporting Information may be found online in the Supporting Information section.

How to cite this article: Nam T-S, Park D-R, Rah S-Y, et al. Interleukin-8 drives CD38 to form NAADP from $NADP^+$ and NAAD in the endolysosomes to mobilize Ca^{2+} and effect cell migration. *The FASEB Journal*. 2020;34:12565–12576. https://doi.org/10.1096/fj.202001249R